Critical Phenomena and Transitions in Swollen Polymer Networks and in Linear Macromolecules

B. Erman* and P. J. Flory

IBM Research Laboratory, San Jose, California 95193. *Received April 2, 1986*

ABSTRACT: The theory of equilibrium swelling and change of dimensions in networks and linear macromolecules is reexamined with the primary object of elucidating the requirements for discontinuous shrinkage through a transition of first order in a poor solvent. The parameter χ that characterizes the solvent–polymer interactions is represented as a function of composition by $\chi = \chi_1 + \chi_2 v_2 + \chi_3 v_2^2 + \ldots$, where v_2 is the volume fraction of polymer. For networks, the elastic free energy is formulated according to current theory of elasticity, which, in contrast to earlier theories, takes account of the nonaffine displacements of network junctions under strain. Coexistence of two phases differing in degree of swelling requires substantial contributions to χ from higher terms in χ_j with $j \geq 2$. The locus of critical points in the χ_1,χ_2 plane, for solvent activity $a_1 = 1$, is examined with $\chi_j = 0$ for $j > 2$ and also for arbitrary values of χ_3. Required values of χ_2 are $\geq 1/3$, the lower limit being reached for vanishing degrees of cross-linking, i.e., for $1/x_c = 0$, where x_c is the (mean) number of segments in a network chain. As x_c decreases, the required value of χ_2 increases and that of χ_1 decreases commencing at $\chi_1 = 1/2$ for $1/x_c = 0$. Requirements for coexistence of two swollen phases in equilibrium with pure solvent (i.e., for $a_1 = 1$) also are explored. Nonpolar solvent–polymer mixtures for which the χ parameters meet the indicated requirements are deemed to be rare. A small proportion of ionized groups on the polymer chain may induce discontinuous shrinkage of the swollen network via a phase transition, as Tanaka and others have shown. The collapse of a randomly coiled linear macromolecule in a poor solvent is susceptible to similar theoretical treatment. Values of the parameters χ_1 and χ_2 required for critical conditions and associated transitions may fall within the range of those found experimentally in real polymer–solvent systems. In particular, the system cyclohexane–polystyrene appears to meet the requirements in this regard. Calculations show that the collapse should occur in this system over a range of ca. 2 °C for a molecular weight of ca. 10^7, in agreement with experiment. Aqueous DNA is an example having the attributes for such behavior as established definitively by the investigations of Post and Zimm.

Introduction

The spatial configuration of a long-chain macromolecule at high dilution in a solvent is determined by the balance between two opposing effects. On the one hand, the segments comprising the chain tend to disperse themselves in the solvent after the manner of the molecules of a solute of low molar mass. The configuration of the macromolecule is thereby dilated so that it pervades a greater volume than would the random, unperturbed chain.[1] On the other hand, the contiguity of the segments required by the chemical bonds that unite them in the macromolecule chain opposes dilation. This effect may be viewed as the elastic response of the polymer chain to deformation—a response that is the basis for the rubber-like elasticity of networks consisting of interconnected polymer chains.

The former effect may be treated as the result of interactions between segments that are proximate in space, although separated by many intervening segments along the polymer chain. In a "good" solvent, these interactions are dominated by the repulsions between the segments that preclude spatial overlap of one by another. Hence, the resulting distortion of the configuration of the polymer chain is customarily designated as the excluded volume effect. The interactions of predominant importance are long range in the topological sense that they involve segments remote in sequence along the chain. In the case of a long chain consisting of "hard" segments, i.e., of segments occupying finite spatial domains but devoid of intermolecular attractions, equivalence of the excluded volume effect to a random walk with avoidance of self-intersections is well established.

Changes of free energy resulting from assemblage of segments in proximity, but at distances such that overlapping is avoided, must also be taken into account.[1,2] These effects are usually treated in terms of the exchange free energy involved in juxtaposing pairs of polymer segments and simultaneously juxtaposing pairs of solvent molecules, these "contacts" between species of like kind being at the expense of those between polymer and solvent. In a "poor" solvent the effective attractions between neighboring segments, expressed by the exchange free energy, may be of a magnitude that compensates the excluded volume repulsions for smaller intersegment distances. At the Θ point the attractions between a pair of neighboring segments precisely counterbalance the volume from which one of them excludes the other, with the result that the excluded volume integral over all distances of separation of the segments vanishes. The spatial configuration of the macromolecule is then unperturbed by the net effects of repulsive and attractive interactions between segments, a situation that finds exact analogy in the Boyle point of a gas. Deeper examination reveals the inadequacy of treating exchange interactions solely in terms of contacts between molecules. Subtle contributions associated with the equations of state of the respective components and of their mixture must be taken into account. This approach is adopted here.

The dilation of the configuration of the linear macromolecular chain associated with the excluded volume effect is closely analogous to the swelling of a macroscopic, three-dimensional polymer network by a diluent.[2,3] Swelling is induced by the tendency of the solvent molecules to disperse in the network, just as a solvent and a solute of low molar mass are induced to mix with one another upon contact. Dilation of the network, however, entails alteration of the configurations of the chains between junctions of the network. They respond elastically, essentially in the manner described above for the isolated linear chain. Swelling equilibrium obtains when these opposing tendencies are in balance. The correspondence to the expansion of a linear polymer chain owing to excluded volume effects is apparent.

* Permanent address: School of Engineering, Bogazici University, Bebek, Istanbul, Turkey.

0024-9297/86/2219-2342$01.50/0

The close similarity between these two effects, the one operating within a single polymer chain and the other in a macroscopic polymer network, has long been recognized. The driving force for dilation is advantageously treated in both cases from the point of view of the theory of mixtures formulated in the framework of classical thermodynamics.[2,3] This approach offers the advantages of generality; it permits comparisons between diverse measurements on the thermodynamics of solutions, on the swelling of polymer networks, and on the spatial dimensions of linear polymer chains in dilute solutions.

In more recent years attention has turned to the behavior of a polymer chain when the effective excluded volume that characterizes the interaction between a pair of segments is negative,[4-7] i.e., when the attractions between neighboring segments dominate repulsive interactions at smaller distances. Under these conditions the region of space pervaded by the random polymer chain must contract to a size smaller than that of the unperturbed chain. If the attractive forces are sufficiently large, one might expect the polymer chain to collapse to a configuration approaching that for dense packing of its segments, with exclusion of the preponderance of the solvent from the domain occupied by the polymer chain. The possibility that the contraction of the polymer chain might occur discontinuously, after the manner of a first-order transition, emerged as an entertaining possibility that has been examined repeatedly.[8]

At the comparatively high densities envisaged for such a contracted state, interactions of higher order than those between pairs of segments must be considered. Ptitsyn, Kron, and Eizner[5] pointed out that truncation of the virial expansion at its second term (which depends exclusively on binary interactions) leads to the palpably false conclusion that a very long macromolecule should collapse to a dense globule, from which all solvent is expelled, when the excluded volume for a segment becomes sufficiently negative. With the inclusion of the third virial term that depends on the third power of the segment concentration, Ptitsyn et al.[5] showed that a substantial quantity of solvent should be retained in the condensed coil. Moverover, the transformation from the random coil to the dense state as the second term in the virial expansion is decreased may, under some conditions, occur discontinuously, i.e., by a transition of first order, although necessarily somewhat diffuse for a system of chains of finite length. They further pointed out that virial terms beyond the third should be taken into account for proper treatment of the transformation from the random coil, in which the mean segment concentration is typically on the order of 1% or less, to the condensed state. de Gennes[7] reaffirmed that continuation of the virial expansion to include the third term in the segment concentration is a minimal requisite for treatment of the self-condensation of a random coil.

Other authors have treated the discontinuous "collapse" of the random coil with reliance on the virial series extended to its third term to express the chemical potential for the mixing of polymer segments with diluent. The theory has been developed on this basis in full detail by Post and Zimm,[9] who showed that the discontinuous contraction of DNA in dilute aqueous solutions containing ethanol in varying proportions is consistent with their theory.

The possibility of phase transitions in networks has been discussed by Dusek and Prins.[10] Recently, Tanaka and Janas as well as Rodriguez and Cohen[11] have observed discontinuous contractions in swollen polyacrylamide gels when the solvent medium is suitably altered. The presence of a small proportion of ionizable units in he polyacrylamide chains was found[12,13] to be essential for discontinuous shrinkage of the gel. The transformation has the characteristics of a phase transition. Analogy to the "collapse" of a linear macromolecule is obvious.

In this paper we reexamine the formulation of the free energy of dilution for networks. Although main emphasis is placed on uncharged networks, we also discuss the case of ionic networks in which a small proportion of ionizable groups modifies the thermodynamic behavior. For nonionic networks, the concentration dependence of the polymer–solvent interaction and the exact form of the mixing term are shown to be of central importance. The inappropriateness of the classical virial expansion, especially at higher polymer concentrations, is pointed out. An alternative formulation, adopted previously for the treatment of the thermodynamics of polymer solutions in general, is employed. In the treatment of the swelling and deswelling of polymer gels advantage is taken of recent developments in the theory of elastic deformation of polymeric networks. The discontinuous contraction of the linear polymer when the solvent medium is suitably varied and the corresponding phase transition in the polymer network are shown to be intimately related. The critical conditions required for manifestation of these phenomena are delineated and they are related to properties that can be ascertained from conventional thermodynamic measurements. In ionic networks, the degree of ionization becomes the dominant factor affecting critical conditions.

Thermodynamic Formulation of the Free Energy of Dilution

The reduced chemical potential $\Delta\tilde{\mu}_1$ for the diluent in admixture with a collection of chain segments connected one to another as in either a coherent network or a single polymer chain may be written[14]

$$\Delta\tilde{\mu}_1 \equiv (\mu_1 - \mu_1^\circ)/RT = \ln(1 - v_2) + v_2 + \chi v_2^2 + (RT)^{-1}(\partial\Delta A_{el}/\partial n_1 + \Delta\mu_i) \quad (1)$$

where v_2 is the volume fraction of polymer segments, assumed uniform throughout the small region considered,[15] χ is the parameter that characterizes the interactions between solvent and polymer,[14,16] ΔA_{el} is the elastic free energy, and n_1 is the number of molecules of the solvent. $\Delta\mu_i$ is the contribution to the total chemical potential by the presence of ionic groups on the chains. The linear additivity of this term in the expression for the chemical potential is valid when the number of ionic groups on each network chain is small. Other symbols have their usual significations. Independent variables other than the composition are the temperature T and pressure p. The first virial term in the number n_2 of polymeric solute molecules is absent inasmuch as eq 1 refers to a solute comprising a fully connected set of segments.[14] We first consider the mixing terms in eq 1, i.e., those that depend explicitly on v_2 in this equation; the elastic and ionic terms will be examined later.

Principal contributions to χ may be estimated from characteristics of the respective components manifested in their equations of state and from the exchange interaction between the solvent and polymer (see below). Insofar as they are significant, inaccuracies[16] in the combinatorial contribution expressed by the first two terms in eq 1, which follow from lattice theory in zeroth approximation (see footnote above), may be absorbed into χ.[17,18] Alternatively, χ may be regarded as an empirical quantity to be evaluated from thermodynamic measurements,[19] e.g., from the osmotic pressure or from the solvent activity a_1 with $\ln a_1 = -\Delta\mu_1/RT$. Proceeding in this fashion, one may

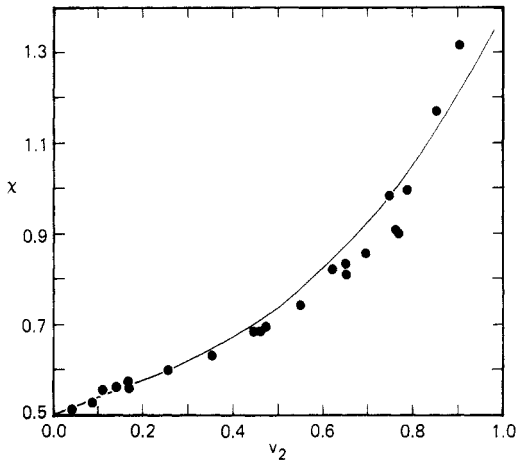

Figure 1. Polymer–solvent interaction parameter χ for cyclohexane–polystyrene plotted as a function of solute volume fraction. Points represent results of experimental measurements of osmotic and vapor pressures[20] at 25 °C. The solid curve is the result of calculations according to equation-of-state theory (see Appendix).

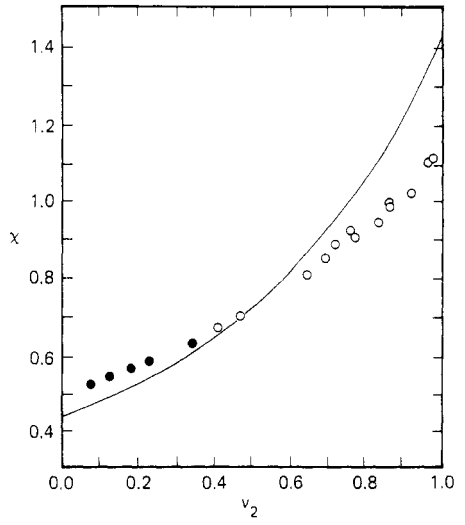

Figure 2. Polymer–solvent interaction parameter χ for benzene–polyisobutylene[21] at 24.5 °C. See legend for Figure 1.

substitute the experimental chemical potential into eq 1 (with the first virial term restored and the elastic term deleted in the case of a linear polymer of finite chain length), which then serves for the empirical evaluation of χ. In general, χ thus determined depends on the composition as well as on the temperature (at constant pressure). It is appropriately expressed empirically by[17,19]

$$\chi = \chi_1 + \chi_2 v_2 + \chi_3 v_2^2 + \dots \quad (2)$$

where χ_1, χ_2, ... are functions of temperature.

Results of experimental measurements of osmotic pressures and vapor pressures treated in this way are shown by the data points in Figures 1 and 2 for the systems cyclohexane–polystyrene (PS)[20] at 25 °C and benzene–polyisobutylene (PIB)[21] at 24.5 °C, respectively. The values of χ deduced from the experimental data according to eq 1 increase with the volume fraction of solute. The latter system was at its Θ temperature, 297.5 K, at which

$$\lim_{v_2 \to 0} \chi = \chi_1 = \tfrac{1}{2}$$

and, hence, the second virial coefficient is zero (see eq 3). The system cyclohexane–PS was 9 K below its Θ point, 307 K; consequently, χ_1 exceeds one-half slightly. The data points (exclusive of those at the highest concentrations for PS) are approximated by

$$\chi = 0.505 + 0.33 v_2 + 0.29 v_2^2$$

for PS in cyclohexane at 25 °C and

$$\chi = 0.500 + 0.30 v_2 + 0.30 v_2^2$$

for PIB in benzene at 24.5 °C. The coefficients χ_2 and χ_3 are subject to uncertainties of ±0.05 and ±0.1, respectively.

The solid lines in Figures 1 and 2 have been calculated theoretically from equation-of-state data as described in the Appendix.

Substitution of eq 2 in eq 1 and series expansion of the logarithmic term yield

$$\Delta\tilde{\mu}_1 = (\chi_1 - \tfrac{1}{2}) v_2^2 + (\chi_2 - \tfrac{1}{3}) v_2^3 + \dots + (RT)^{-1}(\partial \Delta A_{el}/\partial n_1 + \Delta\mu_i) \quad (3)$$

The appeal of this form because of its correspondence to the virial series for the pressure of a gas does not necessarily commend it for application to liquid solutions. The combinatory portion of the chemical potential for a concentrated solution is better represented by the closed expression deduced by lattice methods (i.e., in the present instance by the first two terms of eq 1) than by the virial series truncated after a manageable number of terms. Only for a dilute solution is the expansion in series an acceptable alternative. The advantage of retaining the logarithmic term in the composition finds parallel in the superiority of the ideal solution relationships when applied to mixtures of molecules of comparable size. Arguments on physical grounds requiring the activity to be proportional to $v_1 = 1 - v_2$ in the limit $v_2 \to 1$ confirm that the logarithmic term in eq 1 is exact in this limit. It may be assumed to be approximately valid at lower concentrations v_2 as well. The primary rendition of the combinatory contribution to the free energy should therefore be given preference over series expansion to the virial form.

In the cluster expansion procedure for evaluating the coefficients in the virial series the solvent is treated as a continuum. Its sole effect on the mixture is expressed through the potential of mean force acting between the solute molecules or between polymer segments. Specific characteristics of the components in the liquid state, and the differences between these characteristics for the respective pure components, are ignored. Disregard of the properties peculiar to the respective components is especially serious in the case of a polymer solution in which one of them is a fluid of low molar mass and the other is a polymer of high molecular weight. Owing to the smaller number of intermolecular degress of freedom for unit mass of the latter component, its density considerably exceeds that of the former; its free volume is correspondingly much smaller. These and other differences between the characteristics of the pure components comprising the mixture must affect its properties. Moreover, diverse properties of the mixture, such as its volume and its excess thermodynamic functions, will not, in general, vary linearly with composition, nor can all of them be expected to vary in the same way with composition.

These complications have been largely resolved by formulation of an approximate equation of state that serves to represent both pure components and that can be adapted to embrace mixtures of all compositions.[17,22,23] Quantities used to characterize the respective pure components are their specific volumes $\tilde{v}$, thermal expansivities $\alpha = V^{-1}(\partial V/\partial T)_p$ and thermal pressure coefficients $\gamma = (\partial p/\partial T)_V$.

The essential theoretical relations and their application are summarized in the Appendix. The parameters χ_1 and χ_2 calculated on this basis depend strongly on temperature. Results of calculations for the system cyclohexane–poly-

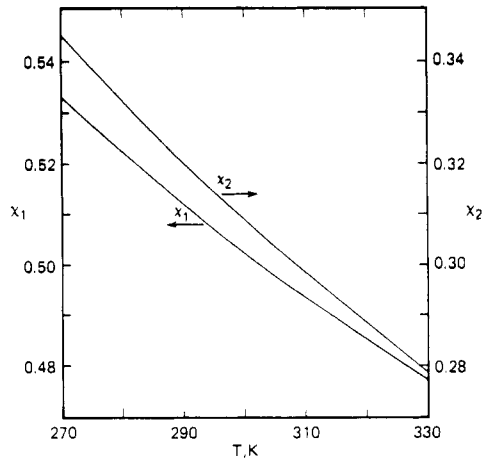

Figure 3. Values of χ_1 (left ordinate) and χ_2 (right ordinate) calculated according to the procedure outlined in the Appendix and plotted as functions of temperature for the system cyclohexane–polystyrene.

styrene are shown as functions of temperature in Figure 3.

Networks

Network Structure and Topology.[24] We consider networks consisting of *linear chains*, each comprising a hundred or more skeletal bonds joined into a network by *multifunctional junctions* connecting the ends of the chains. The number of chains joined by a junction is denoted by the functionality ϕ. Only junctions with $\phi \geq 3$ qualify as multifunctional. Networks with $\phi = 4$, formed by combining pairs of macromolecular chains through cross-linkages, are the ones most frequently considered. If the network is made up of junctions having different functionalities, it may be characterized by its average functionality $\bar{\phi}$.

In a so-called *perfect network*, all ends of the linear chains are attached to multifunctional junctions. In *imperfect networks*, some of the chains are joined to the network at one end only, the other end being unattached. Regardless of whether perfect or imperfect, the networks to be considered are coherent in the graph-theoretical sense. The network may therefore be represented by a connected graph; disconnected fragments, if present, are excluded from consideration.

As the term network implies, closed circuits occur, generally in profusion. The cyclic pathways are delineated by continuous sequences of chemical bonds passing along chains and through junctions. They are random, both in their topological representation and in Cartesian space. Typical networks are characterized by copious interpenetration of their closed circuits, or cyclic paths. They cannot be mapped on a lattice that is replicated through space.

In a perfect network of functionality ϕ (or mean functionality $\bar{\phi}$, the number ν of linear chains is

$$\nu = \phi\mu_J/2 \tag{4}$$

where μ_J is the number of junctions. In the case of a perfect tetrafunctional network, $\nu = 2\mu_J$, where μ_J is the number of tetrafunctional junctions. The network may be characterized by ν or by μ_J and ϕ. The presence of free chain ends in an imperfect network increases the total number ν of chains over the number that would be combined by the μ_J junctions in a perfect network.

From the point of view of its elastic response to deformation, a network, perfect or imperfect, is uniquely characterized by its *cycle rank* ξ, a quantity expressing the number of independent circuits in the network.[24] Otherwise defined, it is the minimum number of scissions required to reduce the network to a coherent tree, i.e., a coherent graph devoid of cyclic connections. For a perfect network

$$\xi = \mu_J(\tfrac{1}{2}\phi - 1) = \nu(1 - 2/\phi) \tag{5}$$

For an imperfect network ξ can be calculated from the stoichiometry and the functionalities of the junctions together with the number of free chain ends. In the sequel we consider only perfect networks. Where specification of the functionality is necessary, the perfect tetrafunctional network will be the prototype.

Elastic Free Energy. We assume that the network was formed from linear macromolecules coexisting in a state of isotropy, in which the molecules are known to occur in their random configurations. The state of reference may then be defined as the state of rest in which the volume V° is such that the chains of the network assume their random, unperturbed configurations at the given temperature. We thus allow for the possibility that the network may have been formed in a diluted system or that the mean dimensions (e.g., $\langle r^2\rangle_0$; cf. seq.) of the unperturbed chains may depend on temperature. In the latter situation the volume V° may depart significantly from the volume at which the network was prepared if the temperature of measurement differs markedly from the temperature prevailing during its preparation.

According to the molecular theory of rubber elasticity,[24,25] the elastic free energy for isotropic dilation by a linear factor λ is given by

$$\Delta A_{el} = (3/2)kT\{\xi(\lambda^2 - 1) + \mu_J(1 + \lambda^2/\kappa)B - \mu_J \ln [(1 + B)(1 + \lambda_2 B/\kappa)]\} \tag{6}$$

where k is the Boltzmann constant,

$$B = (\lambda^2 - 1)/(1 + \lambda^2/\kappa)^2 \tag{7}$$

and λ is the linear dilation ratio defined by

$$\lambda = (V/V^\circ)^{1/3} = (v_2^\circ/v_2)^{1/3} \tag{8}$$

V and V° being the prevailing volume of the network and the volume in the state of reference,[26] respectively; v_2 and v_2° are the corresponding volume fractions of polymer. The parameter κ occurring in eq 6 and 7 measures the constraints on fluctuations of junctions due to the surrounding chains in which they are embedded.[27] It should depend on the degree of interpenetration of the network structure. The number of junctions occurring within the domain pervaded by the ϕ chains emanating from a given junction affords a measure of the interpenetration.[25,28] (Most of the junctions occupying the space thus demarcated are remotely connected to the central one selected.) On this basis one obtains[29]

$$\kappa = I\langle r^2\rangle_0^{3/2}(\mu_J/V^\circ) \tag{9}$$

where $\langle r^2\rangle_0^{1/2}$ is the root-mean-square length of an unperturbed network chain, which serves to define the radius of the region of interpenetration, and I is a numerical constant.

For chains having lengths that are typical in networks ($n > 100$), one may let $\langle r^2\rangle_0 = C_\infty n l^2$, where n is the number of bonds of length l and C_∞ is the characteristic ratio in the limit $n \to \infty$. It will prove expedient to express the length of a chain by the number x_c of segments it contains, a segment being defined as the portion of a chain whose volume equals that of the solvent molecule. Thus

$$n = x_c V_1/\bar{v}M_l$$

where V_1 is the molar volume of the solvent, $\bar{v}$ is the specific volume of the polymer, and M_l is its molecular weight per bond.

For tetrafunctional networks (see eq 5), which are principally considered in the sequel,

$$\mu_J = \nu/2 = v_2^\circ V^\circ N_A/2x_cV_1 \tag{10}$$

where N_A is the Avogadro number. According to experiments on such networks $I \approx {}^1/_2$.[29] Combining these relations, one obtains

$$\kappa = {}^1/_4 P v_2^\circ x_c^{1/2} \tag{11}$$

where the dimensionless parameter P, defined by

$$P = (C_\infty l^2/\bar{v}M_l)^{3/2}V_1^{1/2}N_A = (\langle r^2\rangle_0/x_c)^{3/2}V_1^{-1}N_A \tag{12}$$

depends only on characteristics of the generic type of polymer and on the molar volume of the diluent. It is independent of the junction density in the network, here represented by the inverse quantity x_c.

It is noteworthy that the parameters, ξ and κ or μ_J and κ, occurring in eq 6 for the elastic free energy are fully determined, with the aid of eq 9, by the molecular characteristics of the network as expressed by the degree of cross-linking or by the chain length x_c together with the functionality ϕ.

If constraints on fluctuations of junctions due to their embedment in the welter of surrounding randomly configured chains could somehow be suppressed, then we should have $\kappa = 0$. In this circumstance it would follow that $B = 0$ and the second and third terms in braces in eq 6 vanish; only the first term remains.[25,28] The network thus described would consist of chains manifesting no material properties other than the ability to deliver a force on the junctions to which they are attached, a force that arises from the alterations in their configurations by the strain. A hypothetical network of this description is aptly called a *phantom network*.[24] The first term in eq 6 is therefore identified with the contribution of the phantom network that is the topological analogue of the actual one. A real network approaches its phantom analogue in the limit of high extension and/or dilation.[25,28,29]

At the opposite extreme, fluctuations of the junctions may be considered to be suppressed totally by the constraints, a situation reached if $\kappa \to \infty$. Then $B = \lambda^2 - 1$ and eq 6 becomes[25,28]

$$\Delta A_{el} = (3/2)kT[(\xi + \mu_J)(\lambda^2 - 1) - 2\mu_J \ln \lambda] \tag{13}$$

For a perfect network of any functionality, $\mu_J = 2\nu/\phi$ and $\xi + \mu_J = \nu$. Hence, with the further substitution for λ according to eq 8 we have

$$\Delta A_{el} = kT[(3\nu/2)(\lambda^2 - 1) - (2\nu/\phi) \ln (V/V^\circ)] \tag{13'}$$

This result may be obtained directly for a perfect, *affine network*,[24] i.e., a network in which the junctions are assumed to be firmly embedded in the medium; hence their displacements are linear (or affine) in the macroscopic strain. The logarithmic terms in eq 13 and 13′ account for the dispersion of the embedded junctions over space with dilation. It will be observed that the coefficient (ν) of $(3/2)(\lambda^2 - 1)$ in eq 13′ is twice the coefficient of this term in eq 6 in the case of a perfect tetrafunctional network (for which $\xi = 2\nu$).

Equation 13 or 13′ forms the basis for earlier treatments of swollen networks and the transformations they undergo. The elastic behavior of swollen networks departs markedly from this relationship; it is better represented by the phantom network limit when the network is dilated to the degree that normally occurs in swollen networks. We proceed according to eq 6 with avoidance of approximations attending adoption of either limit.

Ionic Potential. The contribution of ionizable groups to the chemical potential has previously been expressed in its most general form.[2] If the fraction of structural units bearing ionized substituents is very small, their contribution is given by[2,12]

$$(RT)^{-1}\Delta\mu_i = -i\nu(V_1/V^\circ N_A)(v_2/v_2^\circ) \tag{14}$$

where i is the number of ionic groups per chain. Substitution from eq 10 leads to

$$(RT)^{-1}\Delta\mu_i = -iv_2/x_c \tag{14'}$$

Chemical Potential of the Diluent. The elastic contribution $\Delta\tilde{\mu}_{1,el}$ to the reduced chemical potential of the diluent is

$$\Delta\tilde{\mu}_{1,el} \equiv (RT)^{-1}\partial\Delta A_{el}/\partial n_1 = (RT)^{-1}(\partial\Delta A_{el}/\partial\lambda)(\partial\lambda/\partial n_1) \tag{15}$$

where the partial differentiations are to be carried out for a fixed quantity of solute (polymer). Evaluation of the derivatives of eq 6 and 8 gives[30]

$$\Delta\tilde{\mu}_{1,el} = (V_1/N_A V^\circ\lambda)[\xi + \mu_J K(\lambda)] \tag{15'}$$

where

$$K(\lambda) = B[\dot{B}(1 + B)^{-1} + (\lambda/\kappa)^2(B + \lambda^2\dot{B})(1 + \lambda^2 B/\kappa)^{-1}] \tag{16}$$

with

$$\dot{B} = \partial B/\partial\lambda^2 = B[(\lambda^2 - 1)^{-1} - 2(\lambda^2 + \kappa)^{-1}]$$

The linear dilation ratio λ is related to the volume fraction v_2 according to eq 8. With substitution from eq 5 and 10, eq 15′ may be written alternatively as

$$\Delta\tilde{\mu}_{1,el} = (v_2^\circ/x_c)(1 - 2/\phi)\lambda^{-1}[1 + (\mu_J/\xi)K(\lambda)] \tag{15''}$$

which reduces to

$$\Delta\tilde{\mu}_{1,el} = (v_2^\circ/2x_c)\lambda^{-1}[1 + K(\lambda)] \tag{17}$$

for a perfect tetrafunctional network. Substitution of eq 2, 14′, and 15 in eq 1 gives

$$\Delta\tilde{\mu}_1/RT = \ln (1 - v_2) + v_2 + \chi_1 v_2^2 + \chi_2 v_2^3 + \ldots + \Delta\tilde{\mu}_{1,el} - iv_2/x_c \tag{18}$$

for the reduced chemical potential of the diluent in the swollen network.

According to eq 15″, the elastic contribution to the chemical potential of the diluent depends explicitly on the constitution of the network expressed by x_c, ϕ, and v_2°, quantities that represent, respectively, the chain length (reciprocally related to the degree of interlinking), the functionality of the interchain connections, and the reciprocal of the dilation of the network in its state of reference. The elastic contribution depends implicitly on κ, a quantity that is determined by intrinsic characteristics of the polymer chains (see eq 11 and 12) as well as by v_2° and x_c.

Illustrative calculations of the reduced chemical potential according to eq 17 and 18 with $i = 0$ are shown in Figure 4 as functions of the volume fraction for several combinations of parameters. The contribution of $\Delta\tilde{\mu}_{1,el}$, always positive, is dominant at the lowest concentrations. Hence, the reduced chemical potential increases with v_2 initially, causing μ_1 to exceed μ_1° for the pure diluent. If the χ parameters were sufficiently positive (see the series expansion in eq 3) this increase would be sustained with

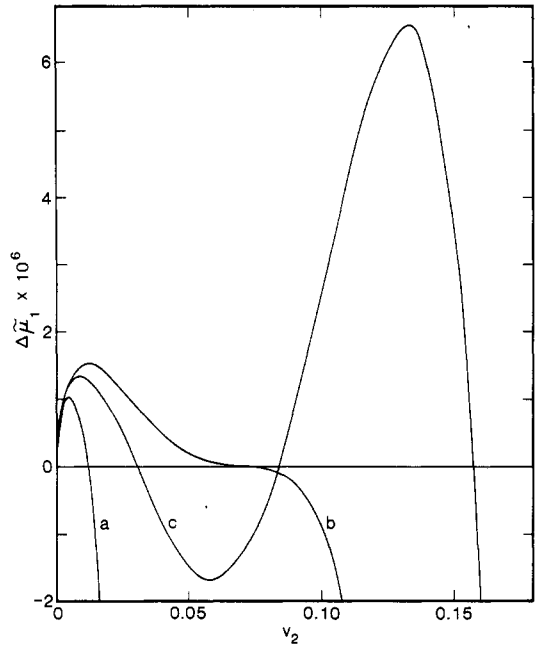

Figure 4. Solvent chemical potentials in swollen networks calculated for $P = 1.5$, $v_2^0 = 1$, $x_c = 10^5$, $\chi_j = 0$ for $j > 2$ and plotted against the solute volume fraction. Curve a: $\chi_1 = 0.49$, $\chi_2 = 0$; curve b: $\chi_1 = 0.4967$, $\chi_2 = 0.3386$; curve c: $\chi_1 = 0.4950$, $\chi_2 = 0.4088$. Curve a illustrates swelling by a good solvent. Curve b depicts a critical point at $\Delta\tilde{\mu}_1 = 0$ and, hence, at coexistence with pure solvent. Curve c shows an instance of triphasic equilibrium between phases with $v_2 = 0$, 0.030, and 0.157.

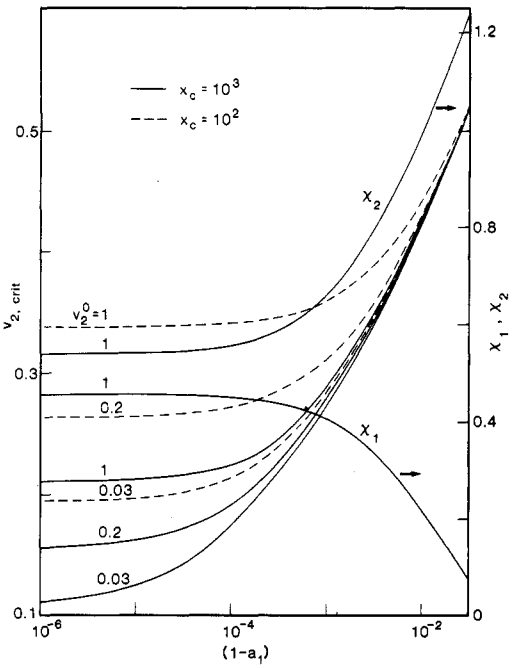

Figure 5. Critical volume fraction $v_{2,crit}$ plotted as a function of $(1 - a_1)$, where a_1 denotes the solvent activity. Results of calculations for $x_c = 10^3$ (solid curves) and for $x_c = 10^2$ (dashed curves) are shown for three different values of v_2^0, all calculations having been carried out with $P = 1.5$ (corresponding to $l = 1.53 \times 10^{-8}$ cm, $C_\infty = 8.5$, $V_1 = 100$ cm^3, and $M_l = 50$). Also shown by curves referred to the right-hand ordinate are values of χ_1 and χ_2 required for critical behavior.

further increase in concentration. If, however, they are small (or negative) the combinatory terms in eq 18 eventually dominate, and $\Delta\tilde{\mu}_1/RT$ becomes negative as shown by curve a in Figure 4. This plot typifies normal swelling behavior in a "good" solvent. The intersection of the abscissa marks the composition for swelling equlibrium with the pure solvent. Curve b has been calculated for a combination of parameters yielding critical behavior at $\Delta\tilde{\mu}_1 = 0$, and curve c is illustrative of separation of the system into two swollen phases in coexistence with pure solvent (see below). The contribution of ionic groups to the total chemical potential of the solvent is negative at all values of v_2. The curves shown in Figure 4, obtained for $i = 0$, are qualitatively unaffected by the presence of ionic groups.

Critical Conditions. At the critical point for a given solvent–polymer system, the first and second derivatives of the chemical potential, taken with respect to composition, vanish. That is, both

$$\Delta\tilde{\mu}'_1 \equiv \partial\Delta\tilde{\mu}_1/\partial v_2 = -v_2(1 - v_2)^{-1} + 2\chi_1 v_2 + 3\chi_2 v_2^2 + \ldots + \Delta\tilde{\mu}'_{1,el} - i/x_c \quad (19)$$

and

$$\Delta\tilde{\mu}''_1 \equiv \partial^2\Delta\tilde{\mu}_1/\partial v_2^2 = -(1 - v_2)^{-2} + 2\chi_1 + 6\chi_2 v_2 + \ldots + \Delta\tilde{\mu}''_{1,el} \quad (20)$$

equate to zero at the critical point. The symbols $\Delta\tilde{\mu}'_{1,el}$ and $\Delta\tilde{\mu}''_{1,el}$ represent the first and second derivatives of $\Delta\tilde{\mu}_{1,el}$ with respect to v_2. They are not expressed algebraically; numerical evaluation will suffice. For a network of specified constitution in interaction with a given diluent, these critical conditions may be fulfilled, at constant pressure, only at a unique temperature and composition.

Realistic examination of critical conditions would require the parameters χ_1, χ_2, ... for the system under investigation and, also, their dependence on temperature. In absence of information in this detail, we may inquire into the values of these parameters that would conduce critical behavior. Inasmuch as volume fractions at activities a_1 approaching unity usually are fairly low (i.e., <0.5), exploratory calculations may be performed with the series in eq 2 truncated at χ_2. Given v_2 and the parameters characterizing the network, as required to evaluate $\Delta\tilde{\mu}_{1,el}$, one may then solve eq 19 and 20, each equated to zero, for χ_1 and χ_2. Substitution in eq 17 for $\phi = 4$, or in eq 15″ for other functionalities, yields the activity $a_1 = \exp(\Delta\tilde{\mu}_1)$ for the chosen value of $v_2 = v_{2,crit}$. In this procedure χ_1 and χ_2 are treated, artificially, as independent parameters whereas, in fact, both are functions of temperature (see Figure 3) and hence related to one another; cf. seq.

Illustrative calculations relating $v_{2,crit}$ to a_1 according to the foregoing procedure are shown in Figure 5 for several tetrafunctional networks having the characteristics indicated in the legend. The calculations shown are confined to the range $0.98 < a_1 \leq 1$. For values of a_1 substantially less than unity, the elastic response of the network is dominated (for $x_c \gg 1$) by mixing interactions. Hence, the curves for diverse networks converge. Calculations in this range ($a_1 \lesssim 0.98$) are of little interest. The values of χ_1 and χ_2 required for critical behavior, also shown in Figure 5, are strongly dependent on the activity. Smooth convergence of the several quantities to their limiting values for $a_1 = 1$ is apparent. We devote foremost attention to this limit in the sequel.

In Figure 6 critical volume fractions $v_{2,crit}$ for $a_1 = 1$ are shown as functions of x_c, the latter being plotted on a logarithmic scale, for several values of the volume fraction $v_2°$ in the state of reference (ordinarily dictated by the volume fraction at which cross-linking was carried out). Dilation in this state, i.e., increase in $1/v_2°$, has the same effect, qualitatively, as a decrease in the degree of interlinking (increase in x_c), as should be expected. In Figure 7, loci of values of χ_1 and χ_2 required for critical conditions are shown for nonionic networks for $\chi_3 = 0$ (solid curve) and for $\chi_3 = 0.25$ (dashed curve). All calculations have

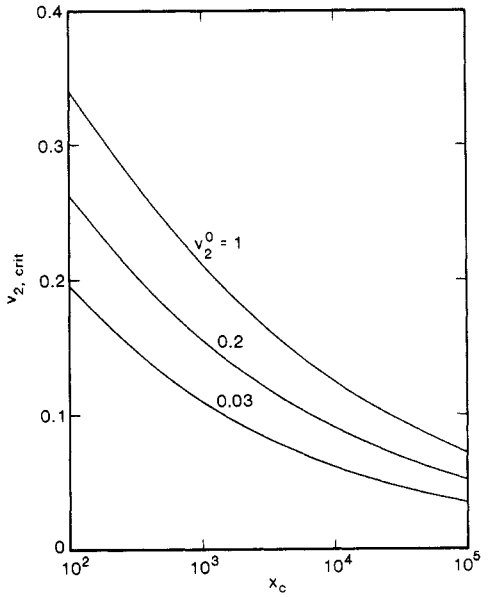

Figure 6. Critical volume fractions $v_{2,crit}$ (for $a_1 = 1$) expressed as functions of x_c for three different values of v_2^0.

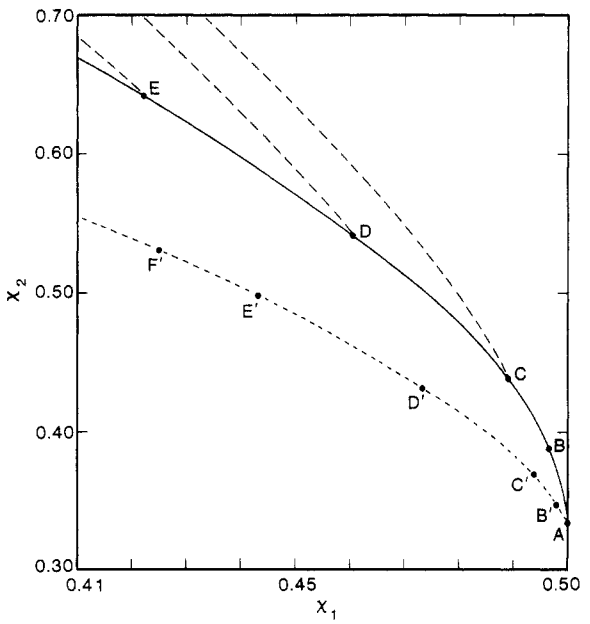

Figure 7. Relationships between χ_1 and χ_2 required for critical behavior (solid and dashed lines) and triphasic equilibria (heavy dashed lines). Points B, C, D, and E refer respectively, to networks with $x_c = 10^5$, 10^4, 10^3, and 3×10^2. Point A is the limiting point for a network with $x_c = \infty$; its coordinates are $\chi_1 = {}^1/_2$, $\chi_2 = {}^1/_3$. The solid and the dashed curves have been calculated for $\chi_3 = 0$ and 0.25, respectively. Points B′, C′, etc. refer to the same values of x_c as A, B, etc. on the solid line. Point F′ is for $x_c = 2 \times 10^2$. The heavy dashed lines leading upward from points C, D, and E indicate values of χ_1 and χ_2 for triphasic equilibrium. All calculations are for $P = 1.5$.

been made for $P = 1.5$. As in the calculations shown in Figure 5, χ_1 and χ_2 are treated as implicit variables. The curves represent loci for the indicated values of x_c. Points B, C, D, and E, for example, represent $x_c = 10^5$, 10^4, 10^3, and 3×10^2, respectively. Extrapolation to $x_c = \infty$ yields point A, at which $\chi_1 = {}^1/_2$ and $\chi_2 = {}^1/_3$. Virtually the same curve is obtained for $v_2^0 < 1$; deviations from the solid line are <0.03% even for $v_2^0 = 0.10$. Values of x_c are altered, however. Thus, for $v_2^0 = 0.10$, points C and D represent networks with x_c having the values 6.65×10^2 and 76, respectively. Values of $v_{2,crit}$ are likewise nearly coincident for various combinations of x_c and v_2^0, yielding a given

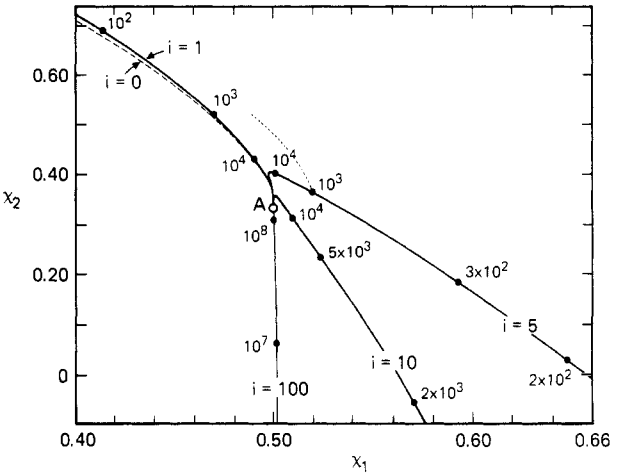

Figure 8. Relationship between χ_1 and χ_2 required for critical behavior in ionic networks. Point A is the limiting point for a network with $x_c = \infty$. Values of i and of representative chain lengths x_c are indicated on each curve. The dashed curve refers to the nonionic network. The dotted curve indicates the values of χ_1 and χ_2 for triphasic equilibrium for a network with $x_c = 10^3$ and $i = 5$. All calculations are for $P = 1.5$.

point on the critical locus. The same critical locus applies in good approximation to phantom networks (for which $\kappa = 0$, i.e., for $P = 0$), and to affine networks ($\kappa = \infty$) with $v_2^0 > 0.2$.

The functional relationship between χ_2 and χ_1 for networks from polymers of a given generic type may intersect the solid curve in Figure 7. This intersection identifies both the constitution (x_c and/or v_2^0) and the temperature (implicit in χ_1 and in χ_2) required for critical behavior at $a_1 = 1$. The constitution of the network, as well as the temperature (at constant pressure), is unique for polymers of the given generic type. If the restriction on a_1 is removed, the variance is increased accordingly; see Figure 5.

In order to explore the effects of higher terms in the series representation of χ, calculations were carried out for $\chi_3 = 0.25$, higher coefficients being zero. The result for the locus of critical points is represented by the dashed heavy curve shown in Figure 7. It falls below the corresponding solid curve for $\chi_3 = 0$; i.e., as expected, lower values of χ_2 are required if $\chi_3 > 0$. The trends of the two curves are similar, however, and they terminate at the same point A. Points B′, C′, etc. refer to the same values of x_c as A, B, etc. on the solid line (see above); point F′ is for $x_c = 2 \times 10^2$.

Figure 8 presents calculations of χ_1 and χ_2 required for critical conditions in ionic networks. Results for $v_2^0 = 1$ and several values of i with $P = 1.5$ are compared (solid curves) with results for nonionic networks (dashed curve). Increasing degrees of ionization alter considerably the conditions for critical behavior. Whereas the required value of χ_1 for nonionic networks is always less than ${}^1/_2$, it generally exceeds ${}^1/_2$ for ionic networks. Required values of χ_2 for ionic networks are also considerably lower than those for nonionic networks under corresponding conditions otherwise.

Close examination of Figure 8 indicates that values of χ_1 and χ_2 required for critical behavior may easily be met by a real polymer–solvent system through adjustment of the cross-link density and/or the degree of ionization. Recent reports[11-13] of observations of transitions in ionized polyacrylamide gels in water–acetone are consistent with these predictions.

Triphasic Equilibria. The calculations presented in Figure 7 show that $\chi_2 > {}^1/_3$ is required for critical coex-

istence of two swollen nonionic network phases together with the pure diluent, regardless of the value of χ_3 (and higher coefficients as well). For physically practicable degrees of interlinking (e.g., for $x_c < 10^3$) a value of $\chi_2 \gtrsim 0.4$ is required. The associated value of χ_1 is somewhat less than 0.50 and it decreases with increase in χ_2 along the critical locus.

The region above the solid line in Figure 7 may be referred to as the triphasic region in which two swollen network phases may coexist with the pure diluent when $\chi_j = 0$ for all $j \geq 3$, provided that necessary conditions are fulfilled. The dashed curve bounds the corresponding region when $\chi_3 = 0.25$ and $\chi_j = 0$ for all $j \geq 4$.

Corresponding triphasic regions for ionic networks are the regions exterior to the convex domain delineated by the critical curves given for several values of i in Figure 8.

Pursuant to a more detailed examination of the triphasic region of the parameter space shown in Figures 7 and 8, we observe that the conditions for such coexistence of two swollen network phases are stipulated by

$$\Delta\tilde{\mu}_1(v_2) = \Delta\tilde{\mu}_1(v_2') = \ln a_1 \tag{21}$$

and

$$\Delta\tilde{\mu}_2(v_2) = \Delta\tilde{\mu}_2(v_2') \tag{22}$$

where v_2 and v_2' are the volume fraction compositions in the coexisting phases and $\Delta\tilde{\mu}_2$ is the reduced chemical potential of an arbitrary subunit of the polymer network, e.g., of a network chain or of a segment thereof. Formulation of this chemical potential is obviated by replacing eq 22 with the equivalent condition

$$\oint_{v_2,v_2'} \Delta\tilde{\mu}_1 \, dn_1 = 0 \tag{22'}$$

where the integration follows the analytical path from v_2 for the more concentrated phase to v_2 for the dilute phase and then returns along the line of equal chemical potential, the quantity of polymer being fixed throughout. If $a_1 = 1$, as is required for triphasic equlibrium, eq 21 is replaced by

$$\Delta\tilde{\mu}_1(v_2) = \Delta\tilde{\mu}_1(v_2') = 0 \tag{23}$$

and eq 22 reduces therefore to

$$\int_{v_2}^{v_2'} \Delta\tilde{\mu}_1 v_2^{-2} \, dv_2 = 0 \tag{24}$$

dn_1 in eq 22 having been replaced by $-n_2 v_2^{-2} \, dv_2$. The integral obtained by substitution of eq 18 in eq 24 may be evaluated numerically.

The heavy dashed lines leading upward from points C, D, and E in Figure 7 for $x_c = 10^4$, 10^3, and 3×10^2, respectively, with $v_2^\circ = 1$ in each instance, have been calculated on the basis of eq 23 and 24. The greater the departure from the critical locus along one of these lines, the greater the magnitude of the biphasic gap (see below). If account is taken of the relationship of χ_2 to χ_1 through their respective dependences on temperature, triphasic equilibrium will be seen to be confined to a unique point on such a curve for a network characterized by given x_c and v_2°. The existence of this point is conditional, of course, on intersection of the χ_1,χ_2 relationship with the dotted line for the given network. The heavy dashed lines in Figure 7 may be regarded as loci for triphasic equilibria in the same sense that the parent solid curve is the locus of critical points, χ_1 and χ_2 being considered as independently variable in both instances.

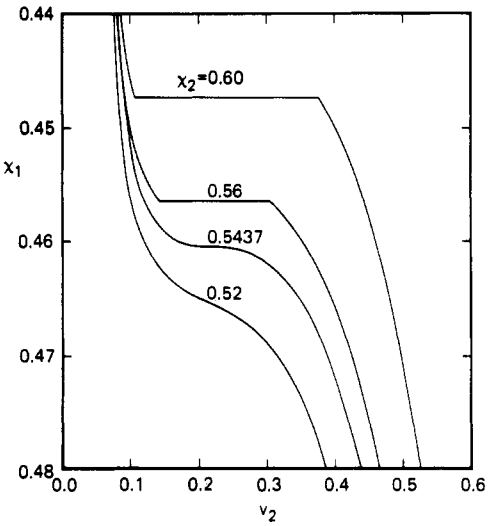

Figure 9. Illustrative calculations of phase equilibria for a network. Curves relate χ_1 to v_2 at swelling equilibrium with solvent for the fixed values of χ_2 indicated on each curve. The curve with $\chi_2 = 0.5437$ represents a network that passes through its critical point as χ_1 is varied. All calculations are for $v_2^\circ = 1.00$, $x_c = 10^3$, and $P = 1.5$.

Similarly, the dotted line in Figure 8 shows the locus of triphasic equilibrium for an ionic network with $i = 5$ and $x_c = 10^3$.

Illustrative calculations of phase equilbria are presented in Figure 9 for a nonionic network with $x_c = 10^3$ and $v_2^\circ = 1.00$, the combination of solvent and polymer being characterized by $P = 1.50$. The curves relate χ_1 to v_2 at swelling equilibrium with the pure solvent for the several values χ_2 indicated. (The implication that χ_2 remains constant while χ_1 varies is unrealistic. The sensitivity of the calculations to χ_1 affords partial justification, however, for treating χ_2 as a constant in these illustrative calculations.) For $\chi_2 < 0.5437$, the critical value, the degree of swelling $1/v_2$ decreases monotonically with increase in χ_1. The latter parameter may be construed as an inverse measure of the temperature. For values of χ_2 exceeding the critical value, triphasic equilibrium occurs at a unique value of χ_1. A value of χ_2 considerably greater than the critical value is required for a large biphasic gap, i.e., for coexistence of two swollen phases differing markedly in composition. As is apparent in Figure 9, the associated values of χ_1 are somewhat smaller.

An increase in the chain length x_c would lower the curves in Figure 9 toward larger values of χ_1. They are lowered also by a decrease in v_2° as is illustrated by the curves in Figure 10 calculated for $x_c = 10^3$ and $v_2^\circ = 0.035$ and referred to the ordinate scale on the left. The pattern of the curves is similar to that for $v_2^\circ = 1$. The interrelated influences of x_c and v_2° are implicit in the generality of the critical locus described above.

Critical Behavior at Low Degrees of Cross-Linking. The interpenetration parameter κ increases with decreasing cross-link density, and the network behavior approaches the affine limit. In this limit, obtained by the substitution of $\kappa = \infty$ into eq 16

$$K(\lambda) = 1 - \lambda^{-2} \tag{25}$$

Upon expanding the logarithmic term up to the fourth order term in eq 18, setting $\chi_j = 0$ for $j > 2$, and using eq 19 and 20, one obtains the following set of equations in the affine limit:

$$\Delta\tilde{\mu}_1 = \left(\chi_1 - \frac{1}{2}\right)v_2^2 + \left(\chi_2 - \frac{1}{3}\right)v_2^3 - \frac{v_2^4}{4} + \frac{(v_2^\circ)^{2/3}}{x_c}v_2^{1/3} - \left(i + \frac{1}{2}\right)\frac{v_2}{x_c} = 0$$

$$\Delta\tilde{\mu}_1' = 2\left(\chi_1 - \frac{1}{2}\right)v_2 + 3\left(\chi_2 - \frac{1}{3}\right)v_2^2 - v_2^3 + \frac{1}{3}\frac{(v_2^\circ)^{2/3}}{x_c}v_2^{-2/3} - \left(i + \frac{1}{2}\right)\Big/ x_c = 0 \quad (26)$$

$$\Delta\tilde{\mu}_1'' = 2\left(\chi_1 - \frac{1}{2}\right) + 6\left(\chi_2 - \frac{1}{3}\right)v_2 - 3v_2^2 - \frac{2}{9}\frac{(v_2^\circ)^{2/3}}{x_c}v_2^{-5/3} = 0$$

Solution of eq 26 for χ_1, χ_2, and v_2 for large x_c leads to

$$v_{2,c} \approx \left[\frac{80}{9}(v_2^\circ)^{2/3}\right]^{3/11} x_c^{-3/11}$$
$$\chi_1 \approx 1/2 \quad (27)$$
$$\chi_2 \approx 1/3$$

These relations become exact in the limit $x_c \to \infty$.

The absence of the ionization parameter i in eq 27 implies convergence of the characteristics of ionic and nonionic gels in the infinite chain length limit.

The Single Chain

Correspondence to the treatment of networks may be achieved through adoption of the smoothed density representation of the polymer chain as a swarm of segments distributed about its center of mass.[1] The form of the distribution of the segments is unimportant for our purposes. It suffices to consider the segments to be uniformly distributed within a sphere of radius proportional to the root-mean-square end-to-end distance of the chain, i.e., equal to

$$\rho_e\langle r^2\rangle^{1/2} = \rho_e\lambda\langle r^2\rangle_0^{1/2} \quad (28)$$

where ρ_e is the constant of proportionality and λ measures the linear deformation of the chain due to self-interactions. The volume fraction of segments within the domain in the unperturbed state is

$$v_2^\circ = 3xV_1/4\pi N_A\rho_e^3\langle r^2\rangle_0^{3/2}$$

This equation may be replaced by

$$v_2^\circ = 3/4\pi\rho_e^3 P x^{1/2} \quad (29)$$

where P is defined by eq 12 with x_c therein replaced by the number x of segments in the linear molecule. The volume fraction in the perturbed state is

$$v_2 = \lambda^{-3}v_2^\circ \quad (30)$$

If, carrying the analogy to network theory further, one relates the elastic free energy to the displacement between the ends of the molecule, then

$$\Delta A_{el} = kT[3(\lambda^2 - 1)/2 - \ln\lambda^3] \quad (31)$$

This relationship may be obtained from eq 13′ upon setting $\nu = 1$ and $\phi = 2$ as for a bifunctional (degenerate) "network". Differentiation of eq 31 gives

$$\Delta\tilde{\mu}_{1,el} = x^{-1}[(v_2^\circ)^{2/3}v_2^{1/3} - v_2] \quad (32)$$

for the elastic contribution to the reduced chemical potential. Equating eq 3 to zero after truncating the series

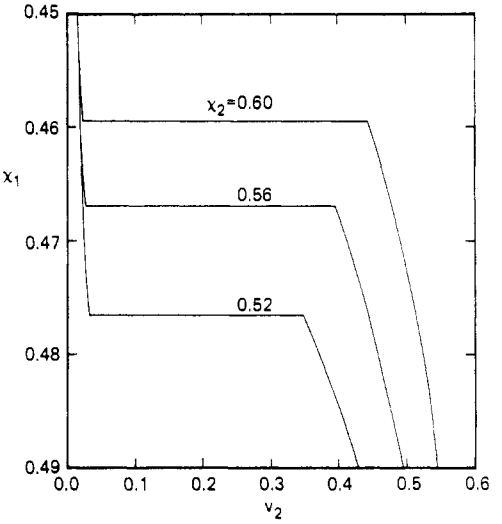

Figure 10. Illustrative calculations of phase equilibria for a network with $v_2^\circ = 0.035$. See legend to Figure 9.

in v_2 at its quadratic (first) term and substituting eq 32 for $\Delta\tilde{\mu}_{1,el}$ therein, one obtains, with the aid of eq 30, the familiar expression[1,2]

$$\lambda^5 - \lambda^3 = C'z \quad (33)$$

for the volume expansion ($\lambda > 1$), or contraction ($\lambda < 1$), due to segment interactions within the randomly coiled macromolecule. In keeping with customary notation, the quantity z is the dimensionless parameter defined by

$$z = (3V_1/\pi N_A)(\langle r^2\rangle_0/x)^{-3/2}x^{1/2}(1/2 - \chi_1) \quad (34)$$
$$= (3x^{1/2}/\pi P)(1/2 - \chi_1) \quad (34')$$

The constant C' is given by

$$C' = 2^{-3/2}(\pi/3)^{1/2}\rho_e^{-3} \quad (35)$$

according to the relationships above.

Agreement with the theory of Fixman[32] for small values of z requires

$$C' = 134/105 \quad (36)$$

from which it follows that

$$\rho_e = (35/268)^{1/3}(3\pi/2)^{1/6} \approx 2/3 \quad (37)$$

Hence

$$v_2^\circ = (6^{1/2}/\pi^{3/2})(67/35)/x^{1/2}P \quad (38)$$

Although the result obtained by substitution of eq 36 in eq 33 is accurate only for $|z| \ll 1$, it provides an approximation that is generally useful even for large values of $|z|$.[33,34] The error in the effective volume fraction v_2° within the unperturbed chain given by eq 38, which rests directly on this approximation, should be inconsequential for the present purpose. Values of v_2° obtained from eq 38 serve both for the evaluation of v_2 according to eq 30, as required for calculation of the chemical potential and its derivatives (see eq 19 and 20), and of the elastic contribution to the chemical potential according to eq 32.

Equations specifying critical conditions for the single chain are obtained by substitution of the first and second derivatives of $\Delta\tilde{\mu}_{1,el}$ with respect to v_2 in eq 19 and 20, respectively. Conditions for triphasic equilibria in the single chain are likewise provided by eq 23 and 24.

Calculations relating $v_{2,crit}$ to a_1 lead to results (not shown) that are qualitatively similar to those for networks shown in Figure 5. Figure 11 corresponds to Figure 7 for networks. As in Figure 7, the solid lines in Figure 11

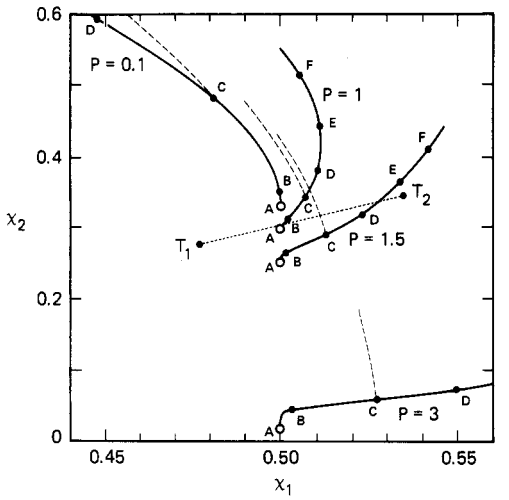

Figure 11. Relationships between χ_1 and χ_2 required for critical behavior (solid lines) and triphasic equilbria (dashed lines) of a single chain for various values of P. The limiting point when $x = \infty$ is indicated by A. Points B, C, D, E, and F refer, respectively, to chains with $x = 10^5$, 10^3, 3×10^2, 10^2, and 50. Triphasic lines are calculated for $x = 10^3$ for each P. The dotted line shows the experimentally determined relationship between χ_1 and χ_2 for the cyclohexane–polystyrene system. Points T_1 and T_2 correspond, respectively, to 270 and 330 K.

represent the loci of critical points for the several values of P indicated in the figure. Although the curve for P = 0.1 resembles the one obtained for networks (compare with Figure 7), increasing the value of P alters these loci markedly. They do not converge to a common point (e.g., to $\chi_1 = {}^1/_2$ and $\chi_2 = {}^1/_3$) in the limit of infinite chain length as found for networks. Points B, C, D, E, and F in Figure 11 refer, respectively, to $x = 10^5$, 10^3, 3×10^2, 10^2, and 50. The dashed lines denote the loci for "triphasic" equilibria for $x = 10^3$. Point A on each curve indicates values of χ_1 and χ_2 in the limit of infinite chain length.

The curves in Figure 11 have been obtained for $\chi_3 = 0$. Nonzero values of χ_3 do not change the positions of the critical loci in an important way, however. Calculations carried out for $\chi_3 = {}^1/_4$ but not shown in Figure 11 indicate that the difference is considerably less than that caused by changes in P. Nonzero values of i induce changes in the critical loci which are qualitatively similar to (but somewhat stronger than) those obtained for ionic networks. They are not reproduced here in interests of brevity.

The relationship between χ_1 and χ_2 obtained according to the equation-of-state formulation for the system cyclohexane–polystyrene is shown by the dotted line in Figure 11. The line has been obtained by taking χ_1 and χ_2 to be functions of temperature as dictated by Figure 3. Points T_1 and T_2 correspond, respectively, to 270 and 330 K. As the temperature is increased, the χ_1,χ_2 parameters change along the dotted line. This line intersects the critical locus for $P = 1.5$, the approximate value of P for polystyrene. It also intersects the triphasic boundary that terminates at point C. This pattern indicates that conditions may be attainable such that polystyrene chains should undergo large changes in dimensions over a small range of temperature. The change may thus resemble a transition.

Results of calculations on the temperature dependence of the dimensions of linear polystyrene chains in cyclohexane are compared with experimental data in Figure 12. The data presented are taken from three independent sources. Filled and empty circles represent light scattering results[35,36] on polystyrene chains with $x = 8.5 \times 10^5$ and 5×10^5, respectively. Triangles represent small-angle

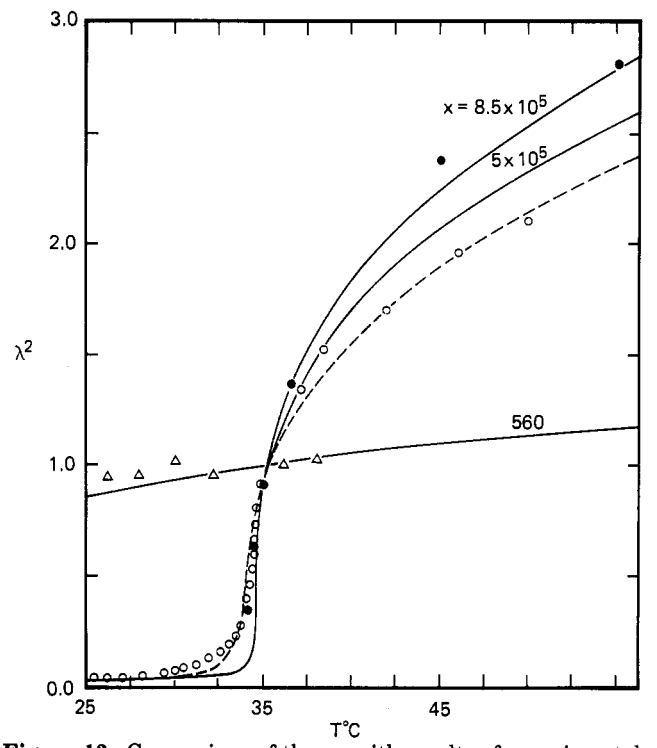

Figure 12. Comparison of theory with results of experimental measurements on dimensions of polystyrene chains in cyclohexane. The ordinate denotes the mean-squared linear expansion. Points show experimental data. Curves have been obtained from the theory. Triangles represent results from ref 37. Filled and open circles are from refs 35 and 36, respectively. Some of the data points from the latter are omitted for interest of clarity.

neutron scattering results[37] on polystyrene chains with x = 560. Solid curves portray calculations from the theory. The ordinate denotes the mean-squared expansion defined by eq 30. Theoretical values of λ^2 have been calculated by equating eq 3 to zero, substituting for $\partial \Delta A_{el}/\partial n$, from eq 32, with $\Delta \mu_i = 0$, and solving for v_2. Equations A-1 and A-2 have been used to obtain χ_1 and χ_2 on the basis of numerical values, cited above, for the equation-of-state parameters. The value of Q_{12} has been reduced by 7.5% below the value of 0.023 J cm^{-3} previously found.[20] This adjustment, which is within the limits of experimental accuracy, was required in order to bring the value of λ to unity precisely at T = 35.4 °C. Values of $v_2°$ have been calculated from eq 38 with $P = 1.5$.

Agreement of theory with experiment for expanded states of the chains is satisfactory. Deviations are within experimental uncertainties as evidenced by comparisons with the two sets of data. For values of $\lambda < 1$, theory agrees with experimental results for short chains (x = 560). However, a marked discrepancy is evident for long chains when $\lambda^2 < 0.5$. The theoretical solid curve exhibits a sharp knee which is not observed in experiments.

The foregoing calculations do not take account of fluctuations of dimensions of individual chains from the mean. Inasmuch as these are small systems, such fluctuations may be substantial. The dashed curve in Figure 12 has been obtained by taking fluctuations into account through Boltzmann averaging of λ^2 over the free energy ΔA given by

$$\Delta A/RT = x(1 - v_2)v_2^{-1}\left[\ln (1 - v_2) + (\chi_1 + \chi_2/2)v_2 + \frac{\chi_2}{2}v_2^2\right] + 3(\lambda^2 - 1)/2 - \ln \lambda^3 + C \quad (39)$$

where C is a constant of integration. The average value of λ^2 is obtained by the use of the expression

$$\langle\lambda^2\rangle = \frac{\int_0^1 (v_2^\circ/v_2)^{2/3} \exp(-\Delta A/kT)\, dv_2}{\int_0^1 \exp(-\Delta A/kT)\, dv_2} \quad (40)$$

The dashed curve in Figure 12 has been obtained for $x = 5 \times 10^5$ with Q_{12} taken 5% below 0.023 J cm^{-3}. This adjustment was required in order to obtain $\langle\lambda^2\rangle = 1$ at $T = 35.4$ °C.

Comparison of the dashed curve with the open circles in Figure 12 shows that averaging in the manner stated above improves the agreement between theory and experiment.

The investigations of Post and Zimm[9] on aqueous solutions of DNA appear to offer the only well-documented instance of a coil–globule transition that may be regarded as discrete and, hence, the analogue of a phase transition. As they point out, characteristics peculiar to this system favor the transition. These characteristics include the stiffnes of the DNA chain, its very high chain length, and interactions peculiar to aqueous media.

Critical Behavior in the Long-Chain Limit. Analyses have been carried out to explore the behavior of the infinitely long chain. Calculations to this end are similar to those carried out according to eq 26 for networks in this limit. After changing x_c in eq 26 to x, replacing $(i + {}^1/_2)$ by $(i + 1)$ as required by the topology of the single chain (i.e., for $\phi = 2$; see statement following eq 31), and deleting the v_2^4 term, which is not required for the case of the single chain, one may solve eq 26, thereby obtaining

$$v_{2,c} \approx Dx^{-1/2}$$

$$\chi_1 \approx {}^1/_2 \quad (41)$$

$$\chi_2 = {}^1/_3 - (i + 1)/4D^2$$

where

$$D \equiv \left[\frac{20}{9}\,\frac{1}{i+1}\right]^{3/2}\left(\frac{3}{4\pi\rho_e{}^3 P}\right) \quad (42)$$

Equation 29 was used for expression of v_2°.

These results show that the critical loci do not converge to the value of $\chi_2 = {}^1/_3$ in the long-chain limit, as in the case of a network. Limiting values of $v_{2,c}$ and χ_2 are strongly affected by ρ_e and P according to eq 41. The first and third equation of eq 41 indicate that, unlike networks, the differences in the behavior of nonionic and ionic chains persist in the long-chain limit.

In the limiting case of infinite chain length, the value of λ at critical conditions is found to be

$$\lambda_c = [9(i + 1)/20]^{1/2} \quad (43)$$

according to eq 29, 30, 41, and 42. For nonionic networks, λ_c in this limit is equal to 0.6708, indicating that the chain size is considerably below its unperturbed magnitude. As is obvious from eq 43, λ_c exceeds the unperturbed value for an ionic chain when i is of the order of unity.

Appendix. Equation-of-State Theory for Binary Mixtures of Solvents and Polymer[17,18,22,23]

According to the theory detailed in the cited references and developed with the specific objective of taking account of the characteristics peculiar to the respective components of the binary mixture, the first two coefficients in the series expansion of χ according to eq 2 are

$$\chi_1 = [({}^1/_2)A^2\alpha_1 + Z_{12})T + Y_{12}](p_1^* V_1^*/\tilde{V}_1 RT) \quad (A\text{-}1)$$

and

$$\chi_2 = \{2(1 - s_2/s_1) \times (Y_{12} + Z_{12}T) + [2Y_{12} + (1 - p_2^* T_1^*/p_1^* T_2^*)A]A\alpha_1 T - (3 + 2\alpha_1 T + 2\alpha_1{}^2 T^2)(2\alpha_1 TA^3/9)\}(p_1^* V_1^*/\tilde{V}_1 RT) \quad (A\text{-}2)$$

where

$$A = (1 - T_1^*/T_2^*)(p_2^*/p_1^*) - (s_2/s_1)X_{12}/p_1^* \quad (A\text{-}3)$$

$$Y_{12} = (s_2/s_1)^2(X_{12}/p_1^*) \quad (A\text{-}4)$$

$$Z_{12} = -Q_{12}(s_2/s_1)^2\tilde{V}_1/p_1^* \quad (A\text{-}5)$$

Quantities appearing in these equations are defined as follows: α_1 is the thermal expansivity of the solvent; V_1^*, p_1^*, and T_1^* are the characteristic volume (hard core), characteristic pressure, and characteristic temperature of the solvent; p_2^* and T_2^* are the corresponding quantities for the solute (polymer); $\tilde{V}_1 = V_1/V_1^*$ is the reduced volume of the solvent; s_2/s_1 is the ratio of surface areas (or contact sites) for a segment of the solute and for a solvent molecule, a segment being defined conveniently as the portion of a solute molecule such that its characteristic volume V_s^* equals that of the solvent molecule, V_1^*; and X_{12} and Q_{12} are the exchange free energy and entropy of interaction, respectively, for formation of a contact between a solute segment and a solvent molecule. The characteristic quantities V^*, p^*, and T^* for the respective components can be calculated from their specific volumes $\bar{v}$, thermal expansion coefficients $\alpha = V^{-1}(\partial V/\partial T)_p$, and thermal pressure coefficients $\gamma = (\partial p/\partial T)_V$ according to the relations[17,23]

$$\tilde{V} = [1 + \alpha T/3(1 + \alpha T)]^3 \quad (A\text{-}6)$$

$$p^* = T\tilde{V}^2\gamma \quad (A\text{-}7)$$

Parameters used for calculation of the curves shown in Figures 1–3 are listed in Table I.

Table I
Parameters Used for Calculation of the Curves in Figures 1–3

	cyclohexane–polystyrene[20]	benzene–polyisobutylene[21]
V_1^*, cm^3	84.3	69.2
T_1^*, K	4717	4710
T_2^*, K	7420	7580
p_1^*, cm^{-3}	530	625
p_2^*, cm^{-3}	547	446
s_2/s_1	0.50	0.58
X_{12}, J cm^{-3}	42	42
Q_{12}, J cm^{-3}	0.023	0
$\alpha_1 \times 10^3$ at 25 °C, K^{-1}	1.217	1.223
$\tilde{V}_1$ at 25 °C	1.291	1.292

References and Notes

(1) Flory, P. J. *J. Chem. Phys.* **1949**, *17*, 303.
(2) Flory, P. J. *Principles of Polymer Chemistry*; Cornell University: Ithaca, NY, 1953; pp 595–602.
(3) Flory, P. J.; Fox, T. G., Jr. *J. Am. Chem. Soc.* **1951**, *73*, 1904.
(4) Stockmayer, W. H. *Makromol. Chem.* **1960**, *35*, 54.
(5) Ptitsyn, O. B.; Kron, A. K.; Eizner, Yu. Ye. *J. Polym. Sci., Part C* **1968**, *16*, 3509.
(6) Domb, C. *Polymer* **1974**, *15*, 259.
(7) de Gennes, P.-G. *J. Phys. (Paris), Lett.* **1975**, *36*, L55.
(8) See, for example: Massih, A. R.; Moore, M. A. *J. Phys. A: Gen. Phys.* **1975**, *8*, 237. Isihara, A.; Isihara, C. H. *Physica (Utrecht)* **1975**, *81A*, 623. Moore, M. A. *J. Phys. A: Gen. Phys.* **1977**, *10*, 305. Naghizadeh, J.; Massih, A. R. *Phys. Rev. Lett.* **1978**, *40*, 1299. Oono, Y.; Oyama, T. *J. Phys. Soc. Jpn.*

1978, 44, 301. Miyakawa, H.; Saito, N. *Polym. J.* **1978**, *10*, 27. Lifshitz, L. M.; Grosberg, A. Yu.; Khokhlov, A. R. *Rev. Mod. Phys.* **1978**, *50*, 683. Malakis, A. *J. Phys. A: Gen. Phys.* **1979**, *12*, 99. Frisch, A. L.; Fesciyan, S. *J. Polym. Sci., Polym. Lett. Ed.* **1979**, *17*, 309. Sanchez, I. C. *Macromolecules* **1979**, *12*, 980.
(9) Post, C. B.; Zimm, B. H. *Biopolymers* **1979**, *18*, 1487; **1981**, *21*, 2123, 2139.
(10) Dusek, K.; Prins, W. *Adv. Polym. Sci.* **1969**, *6*, 1.
(11) Tanaka, T. *Phys. Rev. Lett.* **1978**, *40*, 820. Janas, V. F.; Rodriguez, F.; Cohen, C. *Macromolecules* **1980**, *13*, 978.
(12) Tanaka, T.; Fillmore, D.; Sun, S. J.; Nishia, I.; Swislow, G.; Shah, A. *Phys. Rev. Lett.* **1980**, *45*, 1636.
(13) Ilavsky, M. *Polymer* **1981**, *22*, 1687; **1982**, *15*, 782.
(14) See ref 2, pp 576–581. See also pp 511–514 and pp 520–523.
(15) The often-cited difficulties arising from the nonuniformity of the segment density due to their assemblage in a linear chain are more apparent than real. The quantity required is the probability of occupation of a chosen site in the region, given that vacancy of the sequence of sites required for preceding segments has been established. The conditional probability[16] is somewhat smaller than the a priori probability given by the volume fraction v_2, but the difference is minor.[17] Complication of the equations in order to take account of the conditionality of the probability of occupation of a contiguous site by a polymer segment is disproportionate to the error in use of the a priori probability.
(16) Huggins, M. L. *J. Phys. Chem.* **1942**, *46*, 151; *Ann. N.Y. Acad. Sci.* **1942**, *41*, 1.
(17) Flory, P. J. *Discuss. Faraday Soc.* **1970**, *49*, 7.
(18) Eichinger, B. E.; Flory, P. J. *Trans. Faraday Soc.* **1968**, *64*, 2035.
(19) Flory, P. J.; Daoust, H. *J. Polym. Sci.* **1957**, *25*, 429. Orofino, T. A.; Flory, P. J. *J. Chem. Phys.* **1957**, *26*, 1067.
(20) Höcker, H.; Shih, H.; Flory, P. J. *Trans. Faraday Soc.* **1971**, *67*, 2275.
(21) Eichinger, B. E.; Flory, P. J. *Trans. Faraday Soc.* **1968**, *64*, 2053.
(22) Flory, P. J.; Orwoll, R. A.; Vrij, A. *J. Am. Chem. Soc.* **1964**, *86*, 3515, 3563.
(23) Flory, P. J. *J. Am. Chem. Soc.* **1965**, *87*, 1833.
(24) Flory, P. J. *Proc. R. Soc. London, Ser. A* **1976**, *351*, 351.
(25) Flory, P. J. *J. Chem. Phys.* **1977**, *66*, 5720.
(26) If the network was formed at the temperature of the experiment, v_2^0 is the volume fraction of polymer during network formation. Otherwise, v_2^0 may differ from this volume fraction owing to the temperature dependence (generally small) of V^0; see above. If, as is usual, the network was formed from undiluted polymer and if the change of V^0 with temperature may be ignored, then $v_2^0 = 1$.
(27) In the interest of simplicity we dismiss the additional parameter[28] ζ that takes account of nonlinear distortion under strain of the domains of constraint. Its effect, invariably small, is insignificant in the swollen networks here considered.
(28) Flory, P. J.; Erman, B. *Macromolecules* **1982**, *15*, 800.
(29) Erman, B.; Flory, P. J. *Macromolecules* **1982**, *15*, 806.
(30) Flory, P. J. *Macromolecules* **1979**, *12*, 119.
(31) The virtual coincidence of the critical locus in χ_1,χ_2 for various values of v_2^0 may be understood from the fact that the contributions of the derivatives $\Delta\tilde{\mu}'_{1,el}$ and $\Delta\tilde{\mu}''_{1,el}$ in eq 19 and 20 are relatively small compared to other terms in these equations. Although not negligible, these contributions vary along the critical locus in a manner that causes χ_1 and χ_2 to be determined almost exclusively by $v_{2,crit}$. The functional dependence of χ_2 on χ_1 follows.
(32) Fixman, M. *J. Chem. Phys.* **1955**, *23*, 1656.
(33) Flory, P. J.; Fisk, S. *J. Chem. Phys.* **1966**, *44*, 2243.
(34) Fujita, H.; Norisuye, T. *J. Chem. Phys.* **1970**, *52*, 1115.
(35) Slagowski, E.; Tsai, B.; McIntyre, D. *Macromolecules* **1976**, *9*, 687.
(36) Swislow, G.; Sun, S.; Nishio, I.; Tanaka, T. *Phys. Rev. Lett.* **1980**, *44*, 796. Sun, S.; Nishio, I.; Swislow, G.; Tanaka, T. *J. Chem. Phys.* **1980**, *73*, 5971.
(37) Nierlich, M.; Cotton, J. P.; Farnoux, B. *J. Chem. Phys.* **1978**, *69*, 1379.

Pressure Dependence of Upper Critical Solution Temperatures in Polymer Solutions

S. Saeki,*† N. Kuwahara,‡ K. Hamano,‡ Y. Kenmochi,‡ and T. Yamaguchi†

Department of Polymer Science, Gunma University, Kiryu 376, Japan, and Department of Polymer Engineering, Fukui University, Fukui 910, Japan. *Received February 26, 1986*

ABSTRACT: The pressure dependence of the upper critical solution temperature (UCST) in solutions of polystyrene (PS) in diethyl oxalate (DEO) has been determined over the pressure range 1–1000 atm (1 atm = 0.1011 MPa). The UCST–pressure curves show a minimum when polystyrene has molecular weight $M_w \times 10^{-4}$ = 5.0, 11, and 60, but there is no minimum when $M_w = 1.67 \times 10^4$. The UCSTs increase with increasing pressure over 1–50 atm. The pressure indicating the minimum UCST tends to decrease with decreasing molecular weight of PS. The behavior of the UCST against pressure in PS/DEO has been explained semiquantitatively by the corresponding-states theories by Patterson and Flory, which give a parabolic-like pressure dependence of the χ_1 parameter with a minimum at higher constant temperature and a monotonically increasing function of pressure for χ_1 at lower constant temperature.

Introduction

Investigations of phase separation behavior in polymer solutions over a wide range of temperature up to the vapor–liquid critical point of the solvent[1] have drawn much attention to the theory of polymer solution thermodynamics.[2-4] It is recognized that both upper and lower critical solution temperatures are general phenomena in liquid mixtures and are observed in polymer solutions,[1,5-7] simple liquid mixtures,[8,9] and polymer mixtures.[10] Systematic works have been carried out by introducing pressure as a thermodynamic variable on the critical solution phenomena.[11-19] Over a moderate pressure range, it is observed that the upper critical solution temperature (UCST) for polymer solutions decreases or increases with increasing pressure,[13,15-19] while the lower critical solution temperature (LCST) increases with increasing pressure[11,13,14,16] except for the poly(ethylene glycol)/water system, where LCSTs are almost constant over 1–50 atm.[17] A parabolic-like pressure dependence of the UCST with a minimum is also reported for a few polymer solutions.[19]

The corresponding-states theories derived by Patterson[4] and Flory[2,3] are able to explain the LCST, excess volume of mixing, concentration dependence of the χ parameter, and so on. In this work we have determined the pressure dependence of the UCST in the polystyrene (PS)/diethyl oxalate (DEO) system over the pressure range 1–1000 atm and tried to explain the data with the aid of the corresponding-states theory.

†Fukui University.
‡Gunma University.

0024-9297/86/2219-2353$01.50/0